Gain Optimization of a Near-Field Focusing Array for Hyperthermia Applications

JOSEPH T. LOANE III AND SHUNG-WU LEE, FELLOW, IEEE

Abstract—**A new variation of the array gain optimization problem has arisen in the study of microwave arrays used for hyperthermia, the heating of biological tissue. For a given array configuration and arbitrary medium it is desired to maximize the power deposition at a prescribed focus in the near field of the array. This paper shows how the optimum excitation may be found by solving an eigenvalue problem. Our optimum solution is compared with two other solutions, namely a closed-form solution which optimizes the power in one linear polarization of the radiated field, and a solution based on the popular conjugate-field scheme.**

I. Introduction

A NEW VARIATION of the array gain optimization problem has arisen in the study of microwave arrays used for hyperthermia, the heating of biological tissue. For a given array configuration and arbitrary medium it is desired to maximize the power deposition at the observation point in the near field of the array, analogous to the lossless case of radiation maximization in a particular direction. In this formulation the medium need be neither homogeneous nor lossless, and the array elements need not be identical.

For a given array and desired focus, this paper shows how the optimum excitation may be found to produce maximum power deposition, which is proportional to the specific absorption rate, at a focus in the near field of the array for unit input power. This is a generalization of the far-field formulation of Lo *et al.* [1] in which only one received polarization is maximized. Some practical cases are simulated with both lossy and lossless media, showing that the formulation of [1] gives results that closely follow the optimum when the dominant polarization from linearly polarized radiators is maximized. A comparison is also made with the conjugate-field or time-reversal excitation [2]–[4], a scheme which is slightly less efficient in most cases and which causes significantly higher focal shifts for some off-axis scan situations.

II. Formulation of the Problem

Consider the antenna array of N elements sketched in Fig. 1. We assume a rather general situation such that (i) not all elements are identical, and (ii) the medium is inhomogeneous with scatterers present. We wish to determine the current excitations $\{I_1, I_2, \cdots, I_N\}$ of the N elements to achieve the maximum power deposition at a prescribed focal point F for a fixed input power to the antenna. To this end, let us define the *gain* of the array as the magnitude squared of the total E field at the focus divided by the total input power to the array. The gain g may be written as the ratio of the quadratic forms:

$$g = \frac{\langle ICI^* \rangle}{\langle IRI^* \rangle} \tag{1}$$

where the N-element array is seen as an N-port network with current vector $I\rangle$ directed into the ports. The $N \times N$ real symmetric matrix R is the real part of the mutual impedance matrix; i.e., $R = \mathrm{Re}\ Z$ and the total input power is

$$P_{\mathrm{in}} = \langle IRI^* \rangle = \mathrm{Re}\langle IZI^* \rangle$$

since Z is complex symmetric. The elements of the Hermitian matrix C are

$$C_{mn} = C^*{}_{nm} = V_m \cdot V^*{}_n$$

or, equivalently, $C = V\rangle \cdot \langle V^*$. We define V_n, the element of $\langle V = [V_1, \cdots, V_N]$, as the vector E field at the focus F due to a unit current entering port n with all other ports open-circuited ($I_n = 1$; $I_m = 0$, $m \neq n$). Then the total $|E|^2$ at the focus is

$$|E(F)|^2 = \langle ICI^* \rangle = \langle IV \rangle \cdot \langle V^* I^* \rangle. \tag{2}$$

In summary, the problem at hand is to maximize g in (1) by varying current $I\rangle$.

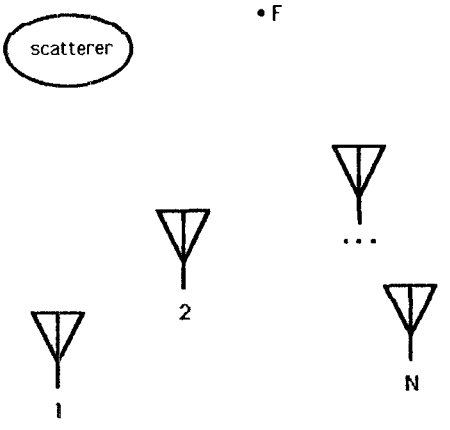

Fig. 1. Arbitrary geometry for general array problem.

Manuscript received December 22, 1986; revised May 26, 1989. This work was supported by the National Science Foundation under Grant ECS-83-11345.

J. T. Loane III is with the Lockheed Missiles and Space Company, Sunnyvale, CA 94088.

S.-W. Lee is with the Electromagnetics Laboratory, University of Illinois, Urbana IL 61801.

IEEE Log Number 8929901.

0018-9480/89/1000-1629$01.00

III. Optimum Gain Solution

Given the desired focus, we want the solution $I\rangle$ to make g stationary with respect to $\delta I\rangle$, which may be found by setting the first variation δg equal to zero. The solution of $I^*\rangle$ is the eigenvector of the generalized eigenvalue problem

$$CI^*\rangle = gRI^*\rangle \tag{3}$$

corresponding to the largest eigenvalue g [5]. This result follows directly from [1, appendix, eq. (22)], with $A = R$ and $\Lambda = 0$. By physical arguments, R is positive definite and C is at least positive semidefinite, so that g from (1) is nonnegative, finite, and real for any observer. In arrays with elements separated by more than about 0.2λ, the mutual resistance matrix R is nonsingular and well conditioned [1]. Therefore, the eigenvalue problem could be written in the standard form $R^{-1}CI^*\rangle = gI^*\rangle$, but (3) is better suited for numerical solution [6]. Standard reduction routines have no trouble solving this equation for practical cases.

IV. Gain Optimization Using One Polarization

A. Linear System Solution

To illustrate, consider the case of electric dipole elements polarized in the x direction. Let the array and the medium both be symmetric such that for an observation point in the yz plane (the H plane), $\Sigma V_{yn} = \Sigma V_{zn} = 0$, where V_{xn}, V_{yn}, V_{zn} are the components of V_n. Fig. 2(a) shows an example of such an array with normal axis z. The optimum gain solution of $I\rangle$ reduces exactly to

$$I^*\rangle = R^{-1}V_x\rangle \tag{4}$$

where $\langle V_x = \langle V \cdot \hat{x} = [V_{x1}, \cdots, V_{xN}]$. This $I^*\rangle$ is the optimum eigenvector of (3) in the H plane by a symmetry argument. Andersen [8] discusses this solution for a focus on the normal axis of an array in the above situation. In the given geometry, the optimum $I\rangle$ must also be distributed symmetrically, so that at the focus

$$\langle IV_y\rangle = \langle IV_z\rangle = 0 \tag{5}$$

$V_x\rangle$, $V_y\rangle$, and $V_z\rangle$ being similarly defined; then the total field $\langle IV\rangle = \hat{x}\langle IV_x\rangle$. The vector $CI^*\rangle$ can be written as

$$\begin{aligned} CI^*\rangle &= V\rangle \cdot \langle V^*I^*\rangle \\ &= V_x\rangle\langle V^*{}_xI^*\rangle + V_y\rangle\langle V^*{}_yI^*\rangle + V_z\rangle\langle V^*{}_zI^*\rangle \\ &= V_x\rangle\langle V^*{}_xI^*\rangle \end{aligned}$$

(5) being the sufficient condition for the last expression. In our geometry, (3) becomes

$$g^{-1}V_x\rangle\langle V^*{}_xI^*\rangle = RI^*\rangle.$$

Since the multiplier of $V_x\rangle$ is a scalar, the optimum eigenvector $I^*\rangle$ is uniquely determined by (4) along with its real eigenvalue:

$$g = \langle V^*{}_xR^{-1}V_x\rangle$$

(or $g = \langle IV_x\rangle$ if $I\rangle$ from (4) has already been calculated).

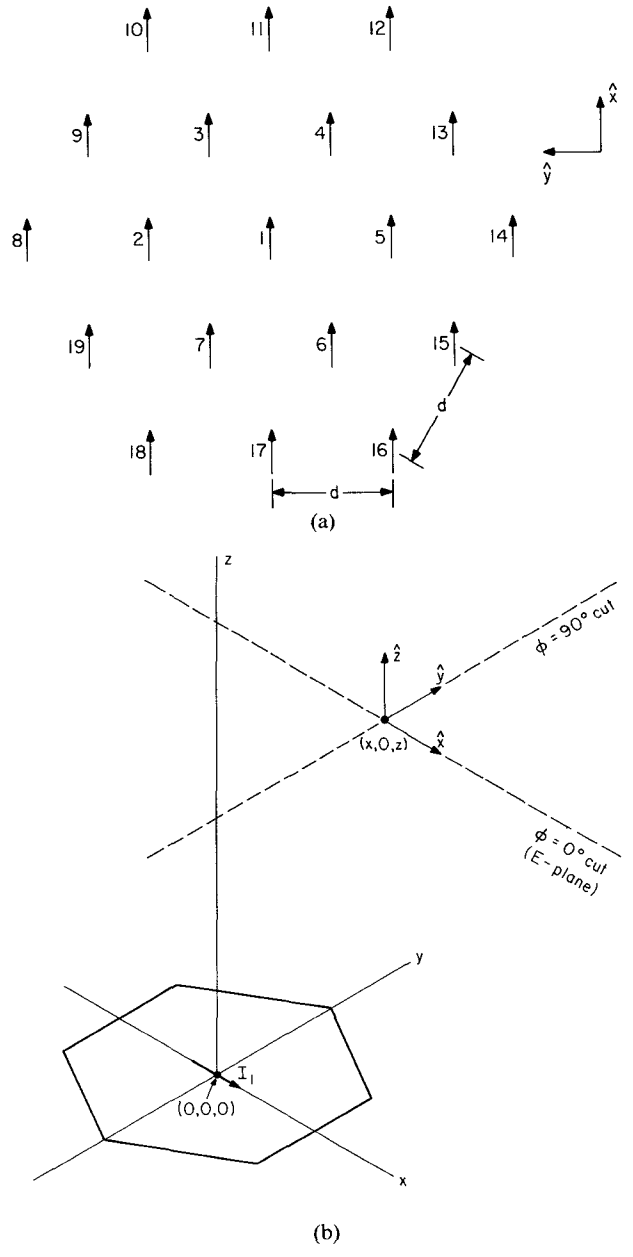

Fig. 2. Focusing array geometry. (a) Equispaced hexagonal array. (b) Pattern cuts.

This formulation is identical to that described by Lo *et al.* [1] for maximizing the directive gain of a conventional array. For a focus in the far field of an array of identical elements, the closed-form matrix solution (4) must approach the optimum as the distance from the source to the focus increases.

Consider a more general array in homogeneous space, whose elements all radiate the same elliptical polarization $(\hat{\theta} + a\hat{\phi})$ in a desired direction (θ,ϕ). Then the optimum solution converges to

$$I^*\rangle = R^{-1}V_\theta\rangle$$

where $\langle V_\theta = \langle V \cdot \hat{\theta} = [V_{\theta 1}, \cdots, V_{\theta N}]$ as the focus recedes to infinity. This is because the vector $CI^*\rangle$ approaches

$$CI^*\rangle = V\rangle \cdot \langle V^*I^*\rangle = (1 + |a|^2)V_\theta\rangle\langle V^*{}_\theta I^*\rangle$$

where $V\rangle = (\hat{\theta} + a\hat{\phi})V_\theta\rangle$. Unit vectors $\hat{\theta}$ and $\hat{\phi}$ are defined by the line from source to focus, and $\{V_{\theta 1}, \cdots, V_{\theta N}\}$ and a are complex scalar quantities.

From (1) through (5), all of our formulation has been exact, but in hyperthermia applications a solution to (3) would be impractical because of the necessity of knowing all three components of V_n. It is simply not possible to know all of the dielectric properties within a particular volume of living tissue. A small probe might be temporarily implanted at the focus in order to obtain enough information about element contributions for a focusing array to be effective. A monopole at the end of a very thin coaxial line is a practical way to do this; a triply polarized implant for UHF wavelengths is probably not feasible. However, a reasonably approximate solution may be had by utilizing the symmetric array example above with a singly polarized receiver. It will be of interest to see how the array focusing ability is affected by looking at patterns and currents when the excitation of (4) is used instead of the optimum. As will be shown, the results of optimizing one dominant polarization follow very closely the optimization of $|\boldsymbol{E}|^2$ even for foci out of the H plane.

B. Conjugate-Field Matching

Another method using one polarization is the conjugate-field (retrodirective, or time-reversal) matching scheme discussed by many authors [2]–[4]. Conjugate-field matching amounts to ignoring mutual coupling in (4), thereby eliminating the requirement of a linear system solution for each desired focus since the matrix R is taken to be diagonal. For identical elements, the solution becomes

$$I\rangle = V^*_x\rangle \tag{6}$$

for dominant x polarization, implying a uniform cophasal distribution in the far-field case. In the near as well as the far field, (6) produces a good but not optimum $|E|^2$ pattern, as we will show by comparison. Of course, the exact matrix R becomes more nearly diagonal as element spacing increases, so that for identical elements the conjugate-field excitation approaches that of (4) for the polarization chosen.

C. Q-Factor and Sensitivity

Another useful parameter which depends on both the array geometry and the excitation is the Q factor [1], defined by

$$Q = \frac{\langle II^* \rangle}{\langle IAI^* \rangle}$$

where A is the resistance matrix due to radiation only; i.e., $\langle IAI^* \rangle$ is the radiated power. For lossless elements $A = R$, and if radiation in a single lossless medium is considered, A is equivalent to the integral $\eta^{-1} \int\int C ds$ over a large sphere. The Q factor is proportional to the total ohmic loss when elements are identical. However, if a case is considered where elements radiate in a lossy medium, the Q factor loses some of its meaning because ohmic loss is distributed in the near field as well as within the elements. The definition of radiation resistance in A becomes rather arbitrary in such a case. In hyperthermia, one would desire a protective "matching section" between array and tissue, either a lossless slab of material or a (lossy) layer of liquid coolant (in which case one might want to integrate $\boldsymbol{E} \times \boldsymbol{H}^*$ over the interface between coolant and tissue).

Perhaps a more useful parameter to compare between different excitations is the sensitivity factor [1], defined as

$$S = \frac{\langle II^* \rangle}{\langle ICI^* \rangle}$$

which does not depend upon A, and which depends on the well-defined input resistance matrix R only indirectly through choice of $I\rangle$. For identical elements, S is proportional to ohmic loss divided by the total $|\boldsymbol{E}|^2$ at the desired focus. S and Q both grow as mutual coupling increases, becoming very large for supergain [1].

V. Numerical Results

By using a far-field approximation for individual element patterns, one can observe qualitative effects on the performance of a focusing array as individual parameters are varied. We have modeled situations for near-field foci with the 19-element x-polarized array shown in Fig. 2. Calculated array patterns for different excitation methods are compared in a lossy medium with a lossless matching section in front of the array. For the model used in approximating the interface effects, refer to the Appendix. The relative permittivities chosen (1 and $1-0.3j$) are simply those of saline body water at around 2 GHz and a reasonable matching section normalized to about $80\epsilon_0$. For the applications we have in mind, the most appropriate pattern cuts are those parallel to the plane of the array.

As in the far-field situation, for element spacings less than about $\lambda/2$ the optimum and matrix-solution gains for near-field focusing are much higher than that of the conjugate field, but for larger element spacings the three excitations all approach the same solution. Near-field focusing produces few nulls, less distinct side lobes, and generally lower grating lobes, since the current distribution is not progressively phased as in far-field beam steering. E-plane scans demonstrate that the differences between matrix solution and optimum excitation are very small. It follows that a monopole probe could be used in practice to optimize array performance. When the array is scanned off-axis, significant focal shifts are predicted for a near-field focus, especially in a lossy medium. The findings are explained below.

An incident $(\cos\theta)^q$ pattern is assumed using identical elements with symmetric E- and H-plane patterns; i.e., $q_E = q_H = q$, so that the relative pattern of an x-polarized element n is

$$V_n \sim \frac{e^{-jkr_n}}{r_n} (\cos\theta_n)^q \left(\hat{\theta}_n \cos\phi_n - \hat{\phi}_n \sin\phi_n\right), \qquad 0 \leq \theta_n < 90^\circ \tag{7}$$

where the subscript n denotes dependence upon element location. For elements less than a whole wavelength across, the far-field approximation should be useful as near as 2λ away [9], [10]. For relative power studies in this paper, we assume lossless elements and let $\eta = 1$, $Q = gS$, and $A = R = \int\int C\,ds$, integrated over a large hemisphere. For integer q, the R matrix of radiation resistance can be computed in closed form, leading to the expressions [7]

$$R_{mn} = 2\pi\left(\frac{\sin\delta}{\delta}\right) \qquad \text{for } q = 0$$

$$R_{mn} = 2\pi\left(\frac{\sin\delta}{\delta^3} - \frac{\cos\delta}{\delta^2}\right) \qquad \text{for } q = 1$$

and

$$R_{mn} = \frac{6\pi}{\delta^2}\left[\left(\frac{3}{\delta^3} - \frac{1}{\delta}\right)\sin\delta - \frac{3}{\delta^2}\cos\delta\right] \qquad \text{for } q = 2$$

where $\delta = kd_{mn}$, the element separation in radians. The wavenumber k must apply to a lossless medium in front of the array with negligible element coupling due to backscatter for this approximation to be worthwhile.

A. Power Decay away from an Aperture

According to the scheme shown in Fig. 2, pattern plots show cuts parallel to the array with $|\boldsymbol{E}|^2$ in decibels on the vertical axis, and wavelengths on the horizontal axis with the focus centered at zero. For an axial focus ($x_f = y_f = 0$), a pattern cut along $\phi = 90°$ lies in the H plane. The origin of the coordinate system coincides with the array center. The elements are numbered as in Fig. 2(b).

Fig. 3 shows power contour plots in the H plane for the same size aperture (2λ diagonal) with different source distributions. The element arrangement in Fig. 2(b) is continued to three rings and a total of 37 elements 0.33λ apart. A 2λ lossless matching section is incorporated, and $|\boldsymbol{E}|^2$ contours are computed 3 dB apart in the lossy region for both optimum (near supergain [1]) and conjugate-field excitations. In such a lossy medium, there is very little difference in the decay rate away from the aperture regardless of the excitation method of an array, implying that little can be done by way of excitation method to decrease surface heating. With conjugate-field excitation, having only 19 elements in the same size aperture leads to practically the same power contours, approximating spherical wave propagation in the medium.

B. Focal Shift

In a lossless medium, the focal shift that occurs for near-field array focusing is on the order of the focal shift observed in front of parabolic reflectors, the latter caused by the geometrical optics divergence factor [9] (see the Appendix) competing with the phase-reinforcement principle. An r^{-1} divergence factor in the near field contributes to a focal shift toward the array. The situation is greatly exaggerated by amplitude decay when the focus is in a lossy medium. For the medium geometry sketched, patterns are shown in Fig. 4 demonstrating the focal shift as the array is scanned from foci at $(2\lambda, 0, 4\lambda)$ to $(4\lambda, 0, 4\lambda)$. A spacing of 0.53λ and an element $q = 2$ were chosen. Lateral focal shift versus off-axis scan distance for a range of foci is plotted in Fig. 5. Note the considerably higher shift for conjugate-field excitation compared to the optimum. For the lossless medium case (not shown), the maximum power level occurs roughly 20 percent closer to the normal axis than the desired focus, and for the two-medium case it occurs roughly 40 percent closer. In Fig. 6 the focal gains for Figs. 4 and 5 are plotted as the focus is moved off-axis, i.e., the optimum gain at focus $(x_f, 0, 4\lambda)$ versus x_f. The corresponding case with $d = 0.8\lambda$ is shown on the same graph.

C. Grating Lobes

Although the excitation is no longer progressively phased for foci in the near field, the distribution is evidently progressive enough to produce grating lobes for certain scan situations. If the element spacing and the angle from the array center to the focus are such that a far-field scan would produce visible grating lobes, then one should at least be cautious in the near field. In Fig. 7, the element spacing is fixed at $d = 0.8\lambda$ and the array is scanned to the focus $(4\lambda, 0, 4\lambda)$, for which isotropic elements exhibit a large grating lobe. While the grating lobe level might be acceptable as far out as focus $(3\lambda, 0, 4\lambda)$, a gain loss of more than 5 dB from axial scan (see Fig. 6) would probably rule out such operation. For focusing near the array axis, grating lobes are not apparent in planar pattern cuts, but their effects are still there, heating the medium closer to the interface. Nevertheless, it would be acceptable to use elements more widely spaced than in a conventional array provided that a satisfactory cooling method existed to pump heat away from the surface.

VI. Conclusions

We have an exact theory of $|\boldsymbol{E}|^2$ gain optimization for a general array focusing in an arbitrary medium. Mutual coupling is accounted for, and elements may be nonidentical, may be placed anywhere, and may have any polarization. However, good results in a practical situation may be obtained with a singly polarized array and copolarized probe.

Accurate $|\boldsymbol{E}|^2$ optimization at a focus is possible using a probe that is singly polarized in the dominant direction. If one can afford it, the most power-efficient system would involve solving N simultaneous equations. The same phase and amplitude measurements are needed for $E_x\rangle$ in both conjugate-field and matrix excitation methods. The slight gain increase possible by monitoring all three polarizations is probably not worth the trouble. We do not consider the possibility of supergain.

Maximizing the power at one point does not imply that that is the maximum power point over a region in space. A hyperthermia array would primarily localize interior heating in planes parallel to the surface. If diseased tissue in a body is at such a location that the array must be scanned, the focal shift described earlier may arise and it would be

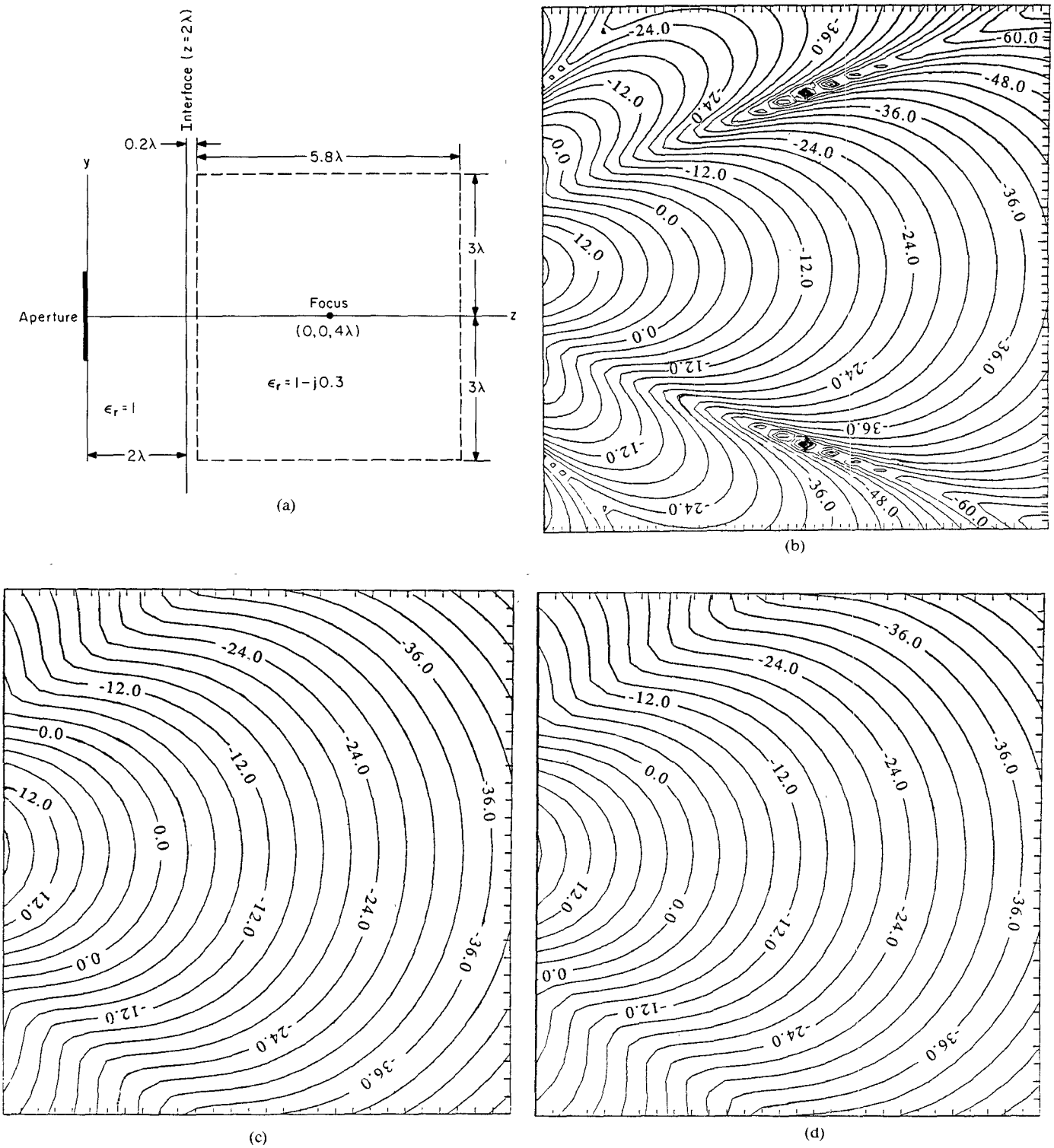

Fig. 3. Power contour plots in the H plane for the sketched medium, in decibels relative to power at focus $(0,0,4\lambda)$. Aperture diagonal 2λ. (a) Medium geometry; (b) 37 elements, $d = 0.33\lambda$, optimum gain, focal power 2.73 dB above (c); (c) 37 elements, $d = 0.33\lambda$, conjugate-field excitation; (d) 19 elements, $d = 0.5\lambda$, conjugate-field excitation, focal power 0.39 dB above (c).

necessary to scan the radiation past the desired focus. Of course, an attempt to scan too far to the side is self-defeating in a lossy medium.

In this study we are interested in heating tissue inside of a body while minimizing the heating on the surface. It is therefore desirable to use a matching section such as the one described to keep the near fields of the elements away from healthy tissue. For deep power penetration it is necessary to take away excess heat at the surface: it is safest to assume that the power level will decrease in any direction away from a practical array, due to the high losses inherent in biological media.

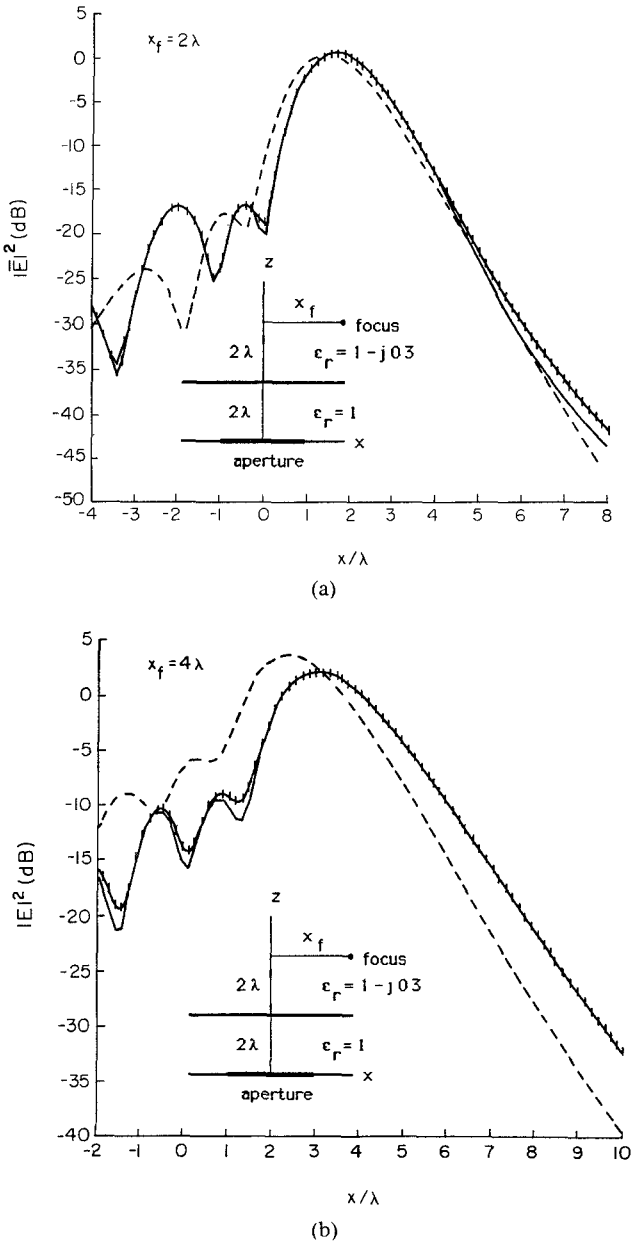

Fig. 4. E-plane $|E|^2$ patterns in the medium sketched for different foci, showing focal shift. Nineteen elements, $d = 0.53\lambda$, $q = 2$, focus = $(x_f, 0, 4\lambda)$, $\phi = 0°$ cut. Optimum gain = solid line; matrix solution = hatched line; conjugate-field = dashed line. (a) $x_f = 2\lambda$; (b) $x_f = 4\lambda$.

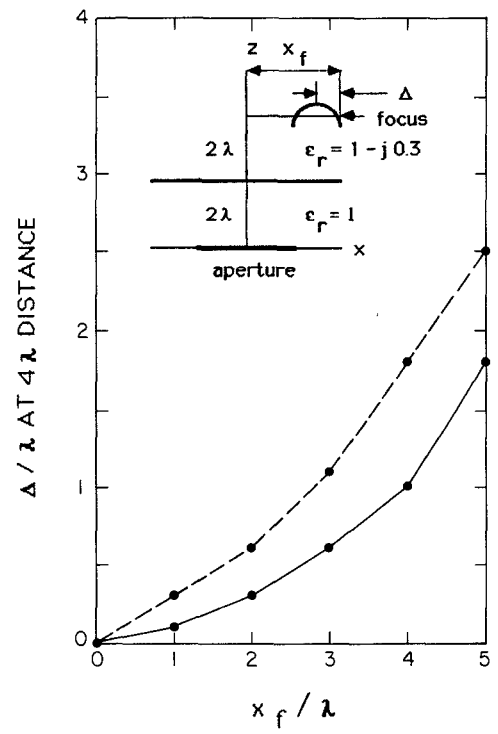

Fig. 5. Lateral focal shift as a function of scan. Nineteen elements, $d = 0.53\lambda$, $q = 2$, focus = $(x_f, 0, 4\lambda)$, $\phi = 0°$ cut Optimum gain = solid line; conjugate-field = dashed line.

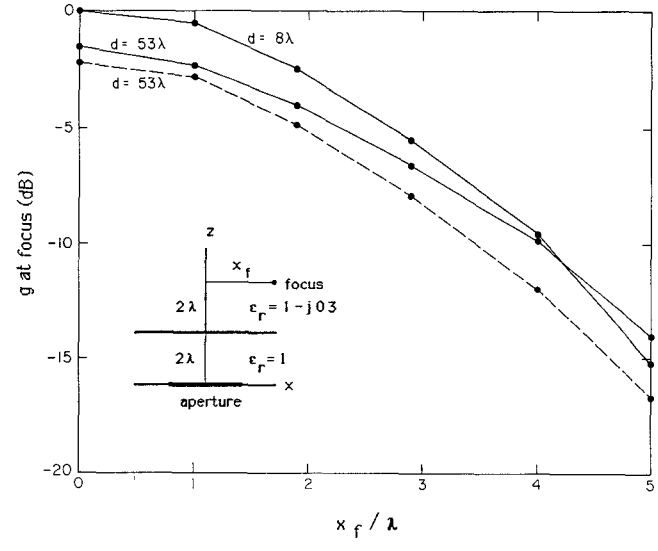

Fig. 6. Focal gain as a function of scan for $d = 0.53\lambda$ and 0.8λ. Nineteen elements. $q = 2$, focus = $(x_f, 0, 4\lambda)$. Optimum gain = solid line; conjugate-field = dashed line. (For $d = 0.8\lambda$ the difference is less than 0.11 dB.)

Appendix

A practical geometrical optics approximation for propagation across an interface between two arbitrarily lossy media has been suggested by Gee *et al.* [7]. Given that a point source in a homogeneous medium of complex k will produce a spherical wave which propagates as $\exp(-jkr)/r$ in the far field, the field behavior appears locally as a plane wave. With the addition of an interface as in Fig. 8, an incident field

$$e^{-jxk_1 \sin\theta_1 - jzk_1 \cos\theta_1}$$

(with θ_1 real) in medium 1 must propagate as

$$e^{-jxk_1 \sin\theta_1 - jz(k_2^2 - k_1^2 \sin^2\theta_1)^{1/2}}, \qquad \mathrm{Im}\left[(k_2^2 - k_1^2 \sin^2\theta_1)^{1/2}\right] \leq 0$$

in medium 2. If we decompose the propagation vector in medium 2 into real and imaginary parts as $\boldsymbol{k}_2 = \boldsymbol{\beta} - j\boldsymbol{\alpha}$, then the amplitude and phase gradients,

$$\boldsymbol{\alpha} = -\hat{x}(\mathrm{Im}\, k_1)\sin\theta_1 - \hat{z}\,\mathrm{Im}\left[(k_2^2 - k_1^2 \sin^2\theta_1)^{1/2}\right]$$

and

$$\boldsymbol{\beta} = \hat{x}(\mathrm{Re}\, k_1)\sin\theta_1 + \hat{z}\,\mathrm{Re}\left[(k_2^2 - k_1^2 \sin^2\theta_1)^{1/2}\right]$$

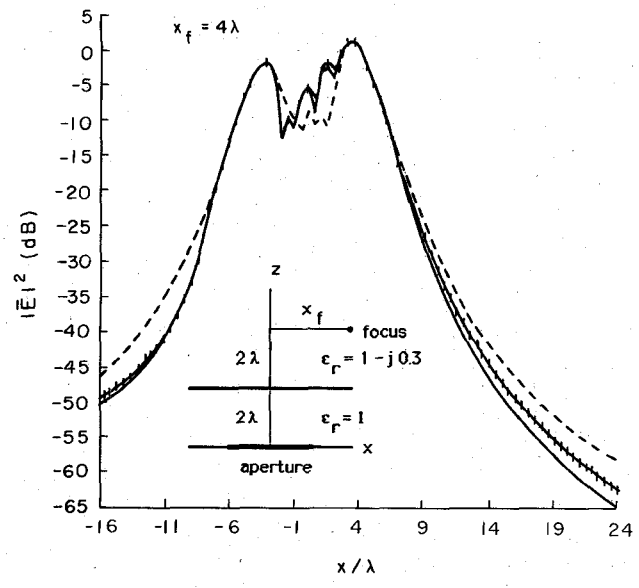

Fig. 7. E = plane pattern in the medium sketched, taken through a grating lobe. Nineteen elements, $d = 0.8\lambda$, $q = 0$, focus = $(4\lambda, 0, 4\lambda)$, $\phi = 0°$ cut. Optimum gain = solid line; matrix solution = hatched line; conjugate-field = dashed line.

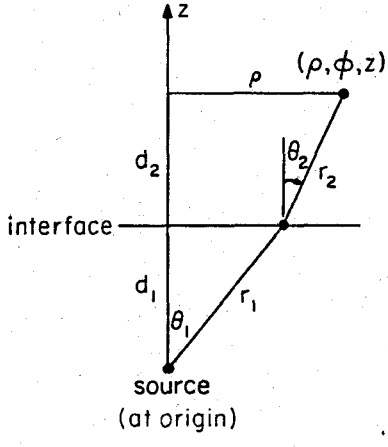

Fig. 8. Definition of ray parameters.

respectively, are not parallel unless $\arg k_2 = \arg k_1$. The approximation used is that the observation point may be taken to be on the vector β; i.e., the phase behavior is retained along k_1 from a point source and then along β. A numerical root-finding method is used to find θ_1, given the source and observation points.

In all geometrical optics applications in this paper, we use the incident field from (7) with standard plane-wave transmission coefficients and a divergence factor [9] which describes the reduction in field strength caused by the spreading of the wavefront between the point just inside medium 2 where the "ray" crosses the interface and the observation point. The divergence factor for the transmitted field is no longer r_1/r, as in a single medium, but is given by

$$(\mathrm{DF}) = \frac{r_1 \tan\theta_1}{\left|\left[\rho\left(\frac{d_1 \tan\theta_1}{\cos^2\theta_1} + \frac{d_2 \tan\theta_2}{\cos^2\theta_2}\right)\right]^{1/2}\right|}$$

where

$$\rho = \sqrt{x^2 + y^2}$$

The angle θ_2 is measured between β and $\hat{z}$.

It can be shown [10] that the above approximation is good for the purposes of this work.

References

[1] Y. T. Lo, S. W. Lee, and Q. H. Lee, "Optimization of directivity and signal-to-noise ratio of an arbitrary antenna array," *Proc. IEEE*, vol. 54, pp. 1033–1045, Aug. 1966.

[2] M. I. Skolnik and D. D. King, "Self-phasing array antennas," *IEEE Trans. Antennas Propagat.*, vol. AP-12, pp. 142–149, Mar. 1964.

[3] B. A. Sichelstiel, W. M. Waters, and T. A. Wild, "Self-focusing array research model," *IEEE Trans. Antennas Propagat.*, vol. AP-12, pp. 150–154, Mar. 1964.

[4] R. N. Assaly and L. J. Ricardi, "A theoretical study of a multi-element scanning feed system for a parabolic cylinder," *IEEE Trans. Antennas Propagat.*, vol. AP-14, pp. 601–605, Sept. 1966.

[5] C. R. Wylie, *Advanced Engineering Mathematics*, 4th ed. New York: McGraw-Hill, 1975, sec. 12.4.

[6] G. Fix and R. Heiberger, "An algorithm for the ill-conditioned generalized eigenvalue problem," *SIAM J. Numer. Anal.*, vol. 9, pp. 78–88, 1972.

[7] W. Gee, S. W. Lee, C. A. Cain, R. Mittra, and R. L. Magin, "Focused array hyperthermia applicator: Theory and experiment," *IEEE Trans. Biomed. Eng.*, vol. BME-31, pp. 38–46, Jan. 1984.

[8] J. B. Andersen, "Theoretical limitations on radiation into muscle tissue," *Int. J. Hyperthermia*, vol. 1, pp. 45–55, 1985.

[9] S. W. Lee, M. S. Sheshadri, V. Jamnejad, and R. Mittra, "Refraction at a curved dielectric interface: Geometrical optics solution," *IEEE Trans. Microwave Theory Tech.*, vol. MTT-30, pp. 12–19, Jan. 1982.

[10] J. Loane and S. W. Lee, "A geometrical optics approximation for refraction at a planar interface between arbitrarily lossy media," *J. Electromag. Waves Appl.*, vol. 1, no. 4, pp. 349–376, 1987.

Joseph T. Loane III was born on June 7, 1951, in Baltimore, MD. He received the B.S. degree in mathematics from Drexel University in 1974. He received the B.S. degree in engineering from San Francisco State University in 1980 and the M.S. and Ph.D. degrees in electrical engineering from the University of Illinois at Urbana-Champaign in 1982 and 1985.

He is currently with the Lockheed Missiles and Space Company, Sunnyvale, CA. His interests lie in the area of electromagnetic theory and include phased arrays, scattering and diffraction, and periodic structures.

Shung-Wu Lee (S'63–M'66–SM'73–F'81) was born in China. He received the Ph.D. degree from the University of Illinois, Urbana, in 1966.

He has been a Professor of Electrical Engineering at the University of Illinois, Urbana, since 1974. Dr. Lee has received a number of awards and citations for his undergraduate teaching.